

## Prey-predator dynamics with periodic solar input - Part II

L. SERTORIO and G. TINETTI

*Dipartimento di Fisica Teorica, Università di Torino - Torino, Italy*  
*Istituto Nazionale di Fisica Nucleare, Sezione di Torino - Torino, Italy*

(ricevuto il 18 Maggio 2000; approvato il 20 Settembre 2000)

**Summary.** — We study a two-component model ecosystem driven by a sinusoidal solar radiation. The governing dynamical system is expressed by two nonlinear differential equations, where the driving term appears factorized to one of the two unknown functions. We show that the solution is asymptotically periodic, with the period of the driving term. Moreover, we find that the asymptotic solution, with the variation of the frequency of the input, shows a resonant-like behaviour. We discuss the interesting similarity between the response of the ecosystem to the external driving term and the response of a genuine resonant system.

PACS 92.60.Ry – Climatology.

PACS 92.70.Gt – Climate dynamics.

PACS 91.10.Vr – Ocean/Earth/atmosphere interaction.

PACS 92.60.Vb – Solar radiation.

### 1. – The governing equations and the asymptotic behaviour

In this paper we consider the dynamical system studied in [1] when the driving term is time dependent, and, in particular, periodic.

Let us recall the governing equations when the driving term is constant [1]. We write

$$(1.1) \quad \begin{cases} \dot{n} = an \left( \mathcal{D} - p \frac{\psi_0}{\phi_0} - n \right) - anp, \\ \dot{p} = -bp + \beta p \left( \frac{\phi_0}{\psi_0} n - p \right). \end{cases}$$

We have used exactly the same symbols as in [1].

We consider now a time-dependent driving term. To this purpose we adopt the

following expression:

$$(1.2) \quad \mathcal{D}(t) = \frac{\phi_{\Delta}^{\max}}{\phi_0} f(t) = \frac{\phi_{\Delta}^{\max}}{\phi_0} \frac{1 - \cos \omega t}{2},$$

where  $\omega$  is assigned. The form of  $f(t)$  given in (1.2) is chosen in such a way that  $\mathcal{D}(t)$  oscillates in the range

$$(1.3) \quad 0 = \mathcal{D}^{\min} \leq \mathcal{D}(t) \leq \mathcal{D}^{\max} = \frac{\phi_{\Delta}^{\max}}{\phi_0} = n^{\max}$$

and  $\mathcal{D} = 0$  for  $t = 0$ ,  $\mathcal{D} = \mathcal{D}^{\max}$  for  $t = \frac{\tau}{2}$ , where  $\tau = \frac{2\pi}{\omega}$ .

The average of  $\mathcal{D}$  over the period  $\tau$  is

$$(1.4) \quad \bar{\mathcal{D}} = \frac{1}{\tau} \int_t^{t+\tau} \mathcal{D}(t') dt' = \frac{n^{\max}}{2}.$$

Moreover, to fix the ideas, we set  $\tau = 24$  h.

Now we insert (1.2) in the dynamical system (1.1) and we get the following system:

$$(1.5) \quad \begin{cases} \dot{n} = an \left( \frac{\phi_{\Delta}^{\max}}{\phi_0} \frac{1 - \cos \omega t}{2} - p \frac{\psi_0}{\phi_0} - n \right) - \alpha np, \\ \dot{p} = -bp + \beta p \left( \frac{\phi_0}{\psi_0} n - p \right). \end{cases}$$

This is the dynamical system that we analyze in this paper. Notice that this system is not autonomous. We wish to show first of all that the solution  $n(t)$ ,  $p(t)$  of (1.5) is asymptotically periodic with the period  $\tau$  of the driving term  $\mathcal{D}$ . To this purpose, we perform the following procedure: we insert into (1.5), in place of  $\mathcal{D}(t)$ ,  $n(t)$ ,  $p(t)$  the averages

$$(1.6) \quad \begin{cases} \bar{\mathcal{D}} = \frac{n^{\max}}{2} \\ \bar{n}(t) = \frac{1}{\tau} \int_t^{t+\tau} n(t') dt' \\ \bar{p}(t) = \frac{1}{\tau} \int_t^{t+\tau} p(t') dt'. \end{cases}$$

In this way we obtain the “segmented system”

$$(1.7) \quad \begin{cases} \dot{\bar{n}} = a\bar{n} \left( \frac{n^{\max}}{2} - \bar{p} \frac{\psi_0}{\phi_0} - \bar{n} \right) - \alpha\bar{n}\bar{p}, \\ \dot{\bar{p}} = -b\bar{p} + \beta\bar{p} \left( \frac{\phi_0}{\psi_0} \bar{n} - \bar{p} \right). \end{cases}$$

The statement that  $n(t)$  and  $p(t)$  are asymptotically periodic is equivalent to the statement that  $\bar{n}(t)$  and  $\bar{p}(t)$  tend to a constant value for  $t \rightarrow \infty$ . Obviously the concept of segmented system makes sense if  $\tau \ll \frac{1}{\alpha}$ , which is our case and theorems 11.5, 11.6 § 11.8 in the book of F. Verhulst.

This is in turn immediately seen if we notice that system (1.7) has a fixed point  $\tilde{\bar{n}}, \tilde{\bar{p}}$  solution of

$$(1.8) \quad \begin{cases} a\bar{n} \left( \frac{n^{\max}}{2} - \bar{p} \frac{\psi_0}{\phi_0} - \bar{n} \right) - \alpha\bar{n}\bar{p} = 0, \\ -b\bar{p} + \beta\bar{p} \left( \frac{\phi_0}{\psi_0} \bar{n} - \bar{p} \right) = 0. \end{cases}$$

Disregarding the trivial case  $\bar{n} = \bar{p} = 0$ , the solution of (1.8) is given by

$$(1.9) \quad \begin{cases} \tilde{\bar{n}} = \frac{\frac{b}{\beta} \left( \frac{\alpha}{a} + \frac{\psi_0}{\phi_0} \right) + \frac{n^{\max}}{2}}{2 + \frac{\alpha}{a} \frac{\phi_0}{\psi_0}}, \\ \tilde{\bar{p}} = \frac{\left( -\frac{b}{\beta} + \frac{\phi_0^{\max}}{2\psi_0} \right)}{2 + \frac{\alpha}{a} \frac{\phi_0}{\psi_0}}, \end{cases}$$

the constants  $\tilde{\bar{n}}, \tilde{\bar{p}}$  are the asymptotic period averages of respectively  $n(t), p(t)$ .

The divergence of the vector flow  $(\dot{\bar{n}}, \dot{\bar{p}})$  (1.7) is negative. System (1.7) can be linearized and we find two eigenvalues with negative real part. This ensures that the fixed point (1.9) is reached either monotonically or with a spiral, in the diagonal basis.

The reader may compare this proof with theorem 2) and relative footnote, in chapter V, § 25, second part, in the book of Arnold and theorems 11.5, 11.6 and 11.8 in the book of F. Verhulst [2]. See also the foregoing sect. 4.

## 2. – The inner parameters

In the dynamical system (1.5) we have  $\omega, \phi_A^{\max}$ , external parameters;  $\phi_0, \psi_0, a, b, \alpha, \beta$ , internal parameters.

Eight parameters affecting a system of two differential equations are evidently too many. We need to search for an underlying logic in this complexity. Let us consider the

couples  $\phi_0, \psi_0$  and  $a, b$ . Some help is given by allometric considerations [3], relating the size of a living organism and its typical mean life. In our case  $\tau_a = \frac{1}{a}$  is the typical time of growth and  $\tau_b = \frac{1}{b}$  is the time of death. In general, the size can be considered proportional to the metabolism and we consider a generic law such that  $\phi_0$  large goes with  $\frac{1}{a}$  large and, analogously,  $\psi_0$  large goes with  $\frac{1}{b}$  large. So we are left with the consideration of small prey and big predator,  $\phi_0 < \psi_0$ ; or big prey and small predator. To summarize this situation, we define a parameter  $z$  in this way:

$$(2.1) \quad \psi_0 = z\phi_0,$$

and, accordingly,

$$(2.2) \quad b^{-1} = za^{-1} \quad \rightarrow \quad b = \frac{1}{z}a.$$

If the linear relationship

$$(2.3) \quad \tau_a \sim \phi_0, \quad \tau_b \sim \psi_0,$$

appears to be too simple, it may be improved, and (2.2) will change accordingly. In the following we choose arbitrarily  $\phi_0 = 0.498 \frac{W}{m^2}$ , so that  $\mathcal{D} = \frac{\phi_{\Delta}^{\max}}{\phi_0} = 700$ . This simply fixes the numerical scale of  $n$ . Due to (2.1),  $\psi_0$  follows.

Concerning  $a$  and  $b$ , we see easily, with the consideration of system (1.5) in the particular case  $p \equiv 0$ , namely

$$(2.4) \quad \dot{n} = an(\mathcal{D}(t) - n),$$

that the parameter  $a$  controls the amplitude of the oscillations of  $n(t)$ . A rigorous discussion of this point is given in sect. 4. Here we take as an obvious fact that a small  $a$  means a small amplitude of oscillation of  $n(t)$ . So, in principle, we may start with a given  $a$ , and  $b$  follows from (2.2).

The presence of the external parameter  $\omega$  fixes a time scale in the numerical calculations. In fact  $\omega$  must be given in certain units of time (for instance  $\text{second}^{-1}$ ,  $\text{hour}^{-1}$ ,  $\text{year}^{-1}$ , etc.) and the parameters of the ecosystem  $a, b, \alpha, \beta$  will be given in units of  $\omega$ . Given  $\omega$ , we may choose an appropriate value for  $a$ . We know from (1.5) that  $a$  gives the growth rate of the prey, we may define  $\tau_a = \frac{2\pi}{a}$  as the time of growth. We assume arbitrarily that  $\tau_a = 200\tau$ , or

$$(2.5) \quad a = \frac{1}{200} \omega = 0.005 \omega.$$

Concerning the coupling constants  $\alpha$  and  $\beta$  we follow the analysis of ref. [1] and we put

$$(2.6) \quad \beta = \beta_{\min} + \frac{\gamma}{1 - \gamma} \alpha,$$

where

$$(2.7) \quad \beta_{\min} = b \frac{2\psi_0}{\phi_{\Delta}^{\max}}$$

and  $0 < \gamma < 1$ .

We will select certain values of  $\gamma$  and analyze the approach to the asymptotic behaviour of  $n(t)$  and  $p(t)$  as a function of the remaining coupling parameter  $\alpha$ .

We focus our attention on the behaviour of system (1.5) in the region of the phase space where the  $\tau$ -average of the predator is maximum, keeping in mind that such region varies with  $\gamma$ .

When  $\tilde{p}$  is maximum, we have

$$(2.8) \quad \frac{d\tilde{p}}{d\alpha} = 0, \quad \gamma \text{ fixed.}$$

Equation (2.8) has the root

$$(2.9) \quad \alpha = \tilde{\alpha}_0 = \frac{2a\psi_0}{\phi_0} \left( \frac{b\phi_0(1-\gamma)}{a\gamma\phi_{\Delta}^{\max}} \right)^{1/2} = 2a \left( \frac{z \frac{\phi_0}{\phi_{\Delta}^{\max}} (1-\gamma)}{\gamma} \right)^{1/2}.$$

We may proceed with the study of the domain of the fixed point  $\tilde{n}, \tilde{p}$ , eq. (1.9) in the phase space  $n, p$ . Each fixed point depends on the eight parameters  $\phi_0, \psi_0, a, b, \alpha, \beta$ , but the boundary of the domain depends only on  $\phi_0, \psi_0$  and  $z$ . In fact the boundary is

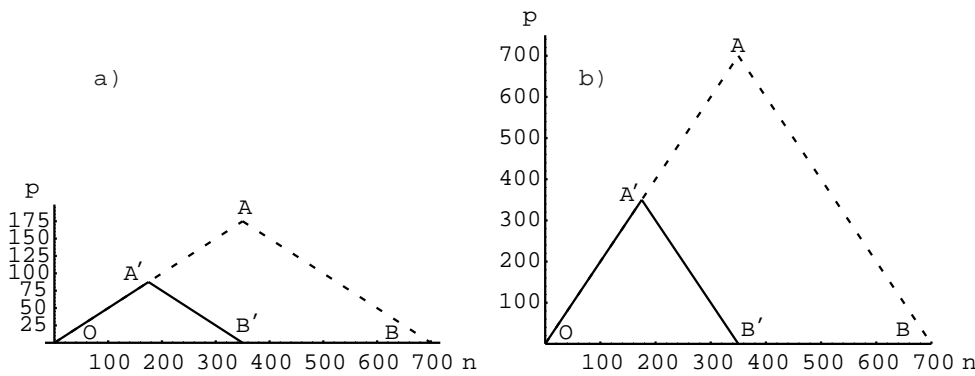


Fig. 1. - Domains of the fixed point  $\tilde{n}, \tilde{p}$  in the phase space  $n, p$  for  $z = 2$  (a) and  $z = 0.5$  (b), where the segment  $A'B'$  belongs to the line:  $\tilde{p} = -\frac{\phi_0}{\psi_0} \tilde{n} + \frac{\phi_{\Delta}^{\max}}{2\psi_0}$  and the segment  $OA'$  to the line  $\tilde{p} = \frac{\phi_0}{\psi_0} \tilde{n}$ . If we choose  $\phi_0 = 0.498 \frac{W}{m^2}$ , we obtain:  $\tilde{n}^{\max} = \frac{\phi_{\Delta}^{\max}}{2\phi_0} = 350$  for both  $z = 2, z = 0.5$ . On the contrary  $\tilde{p}^{\max} = 87.5$  for  $z = 2$ , and  $\tilde{p}^{\max} = 350$  for  $z = 0.5$ . The triangles  $OA, AB$  correspond to the input  $\mathcal{D} = n^{\max}$ , these are the domains discussed in [1]. The triangles  $OA', A'B'$  correspond to the input  $\mathcal{D} = \frac{n^{\max}}{2}$ .

given, according to (1.8), by the two straight lines

$$(2.10) \quad \begin{cases} \frac{n^{\max}}{2} - \bar{p} \frac{\psi_0}{\phi_0} - \bar{n} = 0, \\ \frac{\phi_0}{\psi_0} \bar{n} - \bar{p} = 0. \end{cases}$$

In fig. 1 we show the allowed domain in two cases:

- 1)  $z = 2$ , small prey, large predator,
- 2)  $z = \frac{1}{2}$  large prey, small predator.

### 3. - The transient

The dynamical system (1.5) has two regimes: the transient, which depends on the initial condition  $n(t=0), p(t=0)$ , and the forced asymptotic, which is independent of the initial condition. When we analyze the transient, the interesting question is: how

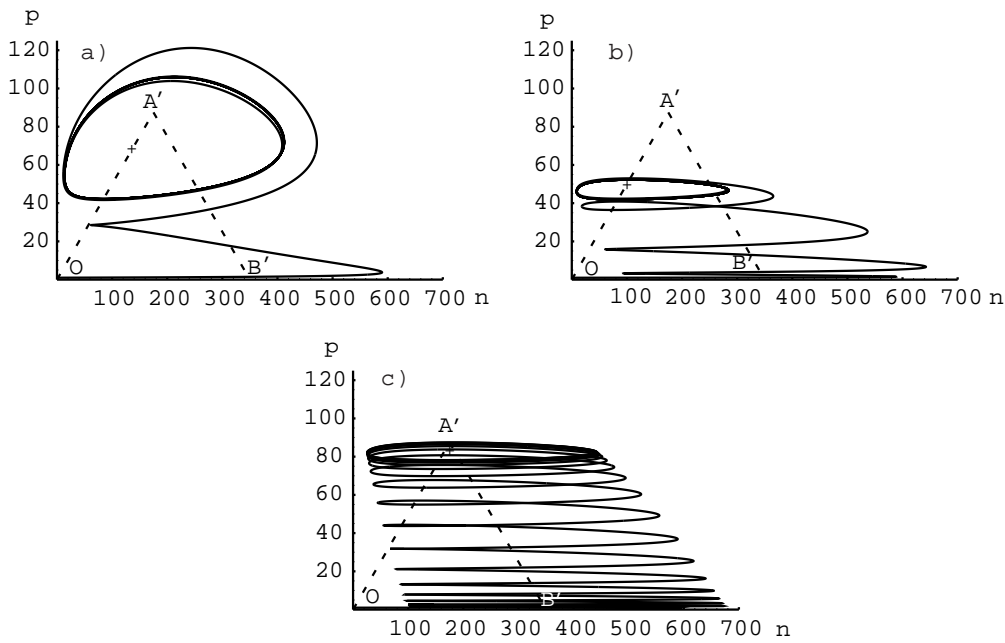


Fig. 2. - In these figures we show three particular trajectories in the phase space  $n, p$ , corresponding to  $z = 2$  and to different values of  $\alpha$  and  $\gamma$ : a)  $\alpha = 10 \hat{\alpha}_0, \gamma = 0.5, z = 2$ ; b)  $\alpha = 10 \hat{\alpha}_0, \gamma = 0.1, z = 2$ ; c)  $\alpha = \hat{\alpha}_0, \gamma = 0.5, z = 2$ . In all the three cases, the initial condition is  $n_0 = p_0 = 1$  and the little cross indicates the asymptotic average values  $\tilde{n}(\alpha, \gamma), \tilde{p}(\alpha, \gamma)$ . Notice that the trajectory intersects itself, since the system is not autonomous. The trajectories a) and b) correspond to very strong coupling. The trajectory c) corresponds to the case in which the predator number is maximum.

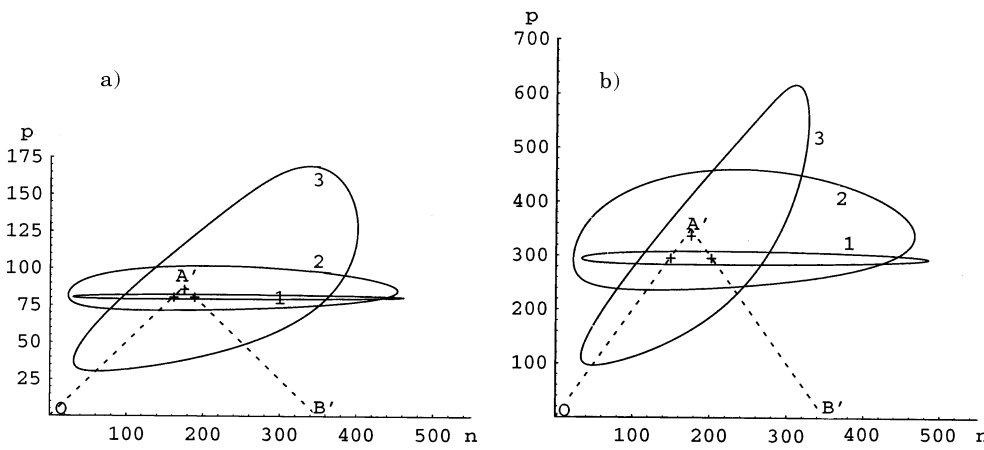


Fig. 3. - In these figures we show three particular trajectories in the phase space  $n, p$ , corresponding to  $z = \frac{1}{2}$  and to different values of  $\alpha$  and  $\gamma$ : a)  $\alpha = 10 \hat{\alpha}_0, \gamma = 0.5, z = 0.5$ ; b)  $\alpha = 10 \hat{\alpha}_0, \gamma = 0.1, z = 0.5$ ; c)  $\alpha = \hat{\alpha}_0, \gamma = 0.5, z = 0.5$ . In all the three cases, the initial condition is  $n_0 = p_0 = 1$  and the little cross indicates the asymptotic average values  $\bar{n}(\alpha, \gamma), \bar{p}(\alpha, \gamma)$ . Notice that the trajectory intersects itself, since the system is not autonomous. The trajectories a) and b) correspond to very strong coupling. The trajectory c) corresponds to the case in which the predator number is maximum.

does the initial condition, namely the “creation” of the ecosystem, affect its evolution? To this purpose, we evaluate numerically two initial conditions:

- 1) the ecosystem begins with a seed  $n(0) = 1, p(0) = 1$ , that we call “minimum creation”;
- 2) the ecosystem begins with a grown prey and only one predator,  $n(0) \sim n^{\max}, p(0) = 1$ , the “creation by steps”.

Are the two initial conditions independent or related? We show in the following figures the evolution of the ecosystem with “minimum creation”, for  $z = 2$ , small predator (fig. 2 and fig. 4) and  $z = \frac{1}{2}$ , large predator (fig. 3). We see that the initial condition with  $p_0 = 1$  and  $n_0 \sim n^{\max}$ , namely prey fully grown, is nothing else than the successive step following the “minimum creation”.

The trajectory with  $\alpha = \hat{\alpha}_0$  and  $\gamma = 0.5$  can be considered the “reference trajectory”: in fact  $\gamma = 0.5$  means  $\beta = \beta_{\min} + \alpha$ , moreover  $\alpha = \hat{\alpha}_0$  means maximum predator.

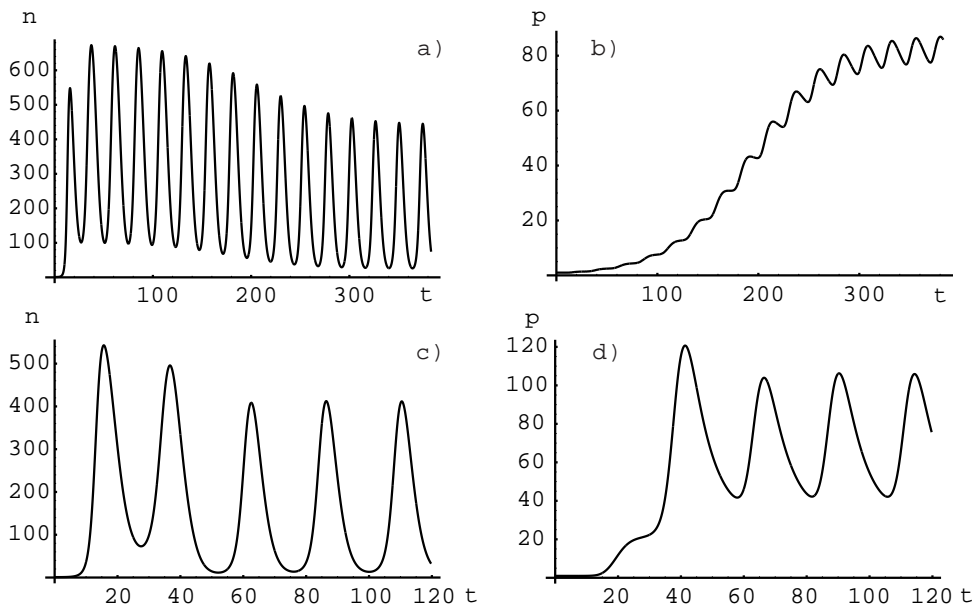


Fig. 4. – In these figures we show the approach to the asymptotic behaviour of  $n(t)$  and  $p(t)$ . The time  $t$  is expressed in hours. The initial condition is  $n_0 = p_0 = 1$ . a) and b) the reference case,  $\alpha = \hat{\alpha}_0$ ,  $\gamma = 0.5$ ,  $z = 2$ . c) and d) the strong coupling case,  $\alpha = 10 \hat{\alpha}_0$ ,  $\gamma = 0.5$ ,  $z = 2$ . Notice that with respect to the reference case, in the strong-coupling case the transient regime is shorter, the amplitude of the oscillation of  $n$  is smaller, and the oscillation of  $p$  is larger.

#### 4. – The asymptotic regime

In general the properties of the asymptotic regime are expressed by the shape and size of the closed curves representing the solution in the phase space, plus the time displacement of the solution with respect to the driving term  $\mathcal{D}(t) = n_{\max} \frac{1 - \cos \omega t}{2}$ .

Once the solution is settled in the asymptotic periodic regime, there is no longer memory of the initial condition that existed in the past. Therefore, we may choose a new origin of time as we wish, since the solution is periodic. We measure the time according to the convention that  $t = 0$  for  $\mathcal{D} = 0$ . With this setting of the clock, we discuss the properties of the solution  $n(t)$ ,  $p(t)$  with respect to the sinusoidal driving term  $\mathcal{D}(t)$  (eq. (1.2)). Notice that the parameters  $\phi_0$ ,  $\psi_0$ ,  $a$ ,  $b$  can be, in principle, determined when a particular couple of species is selected. The parameter  $a$  gives the rate of growth of the prey alone,  $b$  gives the death rate of the predator alone. On the contrary  $\alpha$  and  $\gamma$  are elusive, in the sense that they represent on the macroscopic scale, namely the species numbers, some unknown biological properties of the prey predator coupling on the microscopic scale.

We analyze what happens to the trajectory in the phase space  $n, p$  for  $t \rightarrow \infty$  for  $\gamma$  fixed and when the coupling parameter  $\alpha$  is either smaller or larger than the value  $\hat{\alpha}_0$ ,



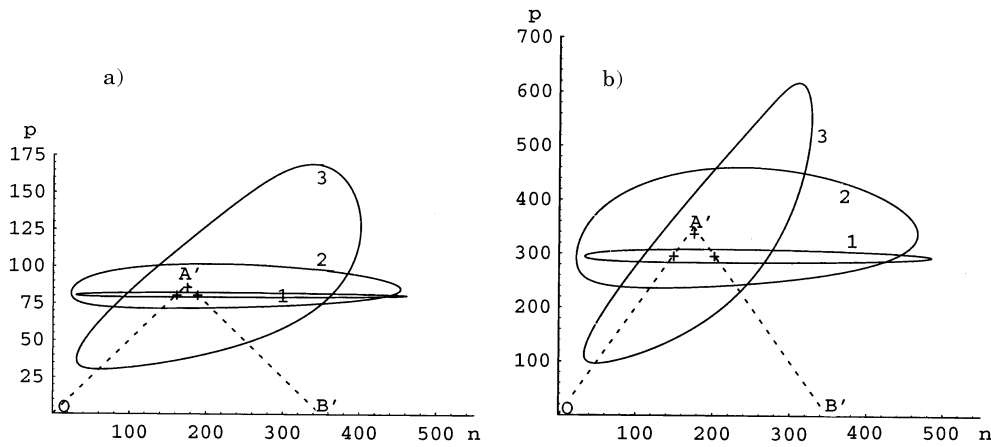


Fig. 5. - Three asymptotic trajectories with  $\gamma = 0.9$ , for  $z = 2$  and for  $z = \frac{1}{2}$ . 1) Weak coupling:  $\alpha = 0.1\hat{\alpha}_0$ , the fixed point is the cross on the right-hand side of A'. 2) Maximum predator:  $\alpha = \hat{\alpha}_0$ , the fixed point is the cross almost coincident with A'. 3) Strong coupling  $\alpha = 10 \cdot \hat{\alpha}_0$ , the fixed point is the cross on the left-hand side of A'.

which is the coupling value giving the maximum value  $\tilde{p}^{\max}$ . We show the results in fig. 5. The amplitude of the predator oscillation is smaller when the coupling is weak (smaller than  $\alpha_0$ ), and keeps increasing for increasing  $\alpha$ . Moreover the trajectory is nearly elliptic for  $\alpha \leq \alpha_0$ , and becomes deformed for  $\alpha > \alpha_0$ .

We observe that only for the trigonometric functions the concept of time displacement appears as a phase shift. In our case  $n(t)$  and  $p(t)$  are periodic, but not sinusoidal, therefore the time displacement needs to be defined in some operational way. We adopt as definition of time displacement  $\mathcal{D} - n$ , the distance in hours between the time at which  $n$  is maximum and the time at which  $\mathcal{D}$  reaches the first maximum after  $\mathcal{D} = 0$ . The same definition applies to the time delay  $n - p$  (fig. 6).

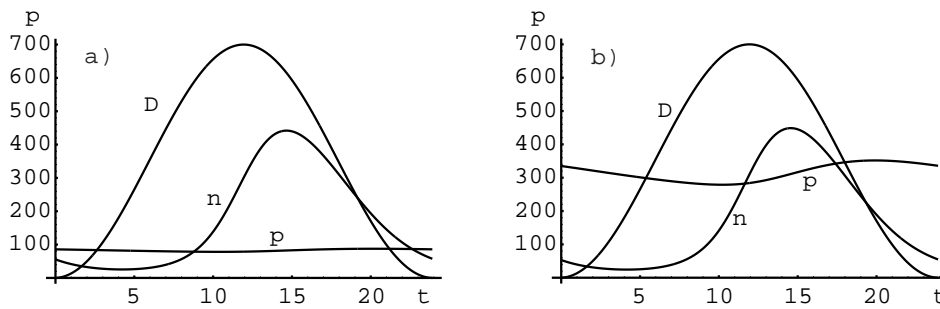


Fig. 6. - Asymptotic regime in the reference case:  $\alpha = \hat{\alpha}_0$ ,  $\gamma = 0.5$ , for  $z = 2$  and for  $z = \frac{1}{2}$ . The solutions of the equation of motion,  $n(t)$  and  $p(t)$ , are compared to the input term  $\mathcal{D}(t)$  (eq. (1.2)). Time is expressed in hours.

### 5. – The linearization and perturbation

We said, at the beginning of the preceding section, that the properties of the asymptotic solution are: shape, size, and time displacement. In that section we have presented a set of figures that show numerically how these properties depend on  $z$  and  $\alpha$ .

Now we wish to understand analytically (not numerically) how these properties depend on the inner parameters. This can only be done by a process of linearization, whereby the system can be solved analytically. There is a cost in such approach: we miss the property of shape, as the solutions of a linear system driven by a sinusoidal term are also sinusoidal; in other words the shape is given *a priori*, we can only dig on amplitude and displacement. Moreover, we must be aware that in the process of approximating a periodic nonlinear solution with a sinusoid, we may violate the request  $n(t) > 0$ ,  $p(t) > 0$ . This request is embedded in the dynamical system (1.5) and is obvious: negative numbers  $n$  and  $p$  are meaningless. Therefore, we need to reset the formalism appropriately. For the discussion of the linearization, we introduce a perturbation parameter  $\varepsilon$ , running in the interval  $0 \leq \varepsilon \leq 1$ , multiplying  $\cos \omega t$ , so that we start with the dynamical system

$$(5.1) \quad \begin{cases} \dot{n} = an \left( \frac{\phi_A^{\max}}{\phi_0} \frac{1 - \varepsilon \cos \omega t}{2} - p \frac{\psi_0}{\phi_0} - n \right) - \alpha np, \\ \dot{p} = -bp + \beta p \left( \frac{\phi_0}{\psi_0} n - p \right). \end{cases}$$

Furthermore we like to deal with an autonomous system. This is easily obtained at the cost of introducing an extended phase space with two additional dimensions for the two variables  $q(t)$  and  $r(t)$ , which together with  $n(t)$  and  $p(t)$  satisfy the “extended system”:

$$(5.2) \quad \begin{cases} \dot{n} = an \left( \frac{\phi_A^{\max}}{\phi_0} \frac{1 - \varepsilon q}{2} - p \frac{\psi_0}{\phi_0} - n \right) - \alpha np, \\ \dot{p} = -bp + \beta p \left( \frac{\phi_0}{\psi_0} n - p \right), \\ \dot{q} = r, \\ \dot{r} = -\omega^2 q. \end{cases}$$

Clearly the third and the fourth equations in (5.2), with initial conditions  $q(t=0) = 1$ ,  $r(t=0) = 0$ , produce the solution

$$(5.3) \quad \begin{cases} q(t) = \cos \omega t, \\ r(t) = -\omega \sin \omega t, \end{cases}$$

and therefore (5.2) is the right extension of system (5.1). System (5.2) is autonomous and we can study the topology of the flow  $n(t)$ ,  $p(t)$ ,  $q(t)$ ,  $r(t)$  in the 4-dimensional phase space. The role of the parameter  $\varepsilon$  will be discussed in the following. We show first of

all that (5.2) has only one fixed point ( $n > 0, p > 0$ ) solution of

$$(5.4) \quad \begin{cases} \alpha n \left( \frac{\phi_{\Delta}^{\max}}{\phi_0} \frac{1 - \varepsilon q}{2} - p \frac{\psi_0}{\phi_0} - n \right) - \alpha n p = 0, \\ -bp + \beta p \left( \frac{\phi_0}{\psi_0} n - p \right) = 0, \\ -\omega^2 q = 0, \\ r = 0. \end{cases}$$

The solution of (5.4) is

$$(5.5) \quad \begin{cases} \widehat{n} = \frac{\frac{b}{\beta} \left( \frac{\alpha}{a} + \frac{\psi_0}{\phi_0} \right) + \frac{\phi_{\Delta}^{\max}}{2\phi_0}}{2 + \frac{\alpha}{a} \frac{\phi_0}{\psi_0}}, \\ \widehat{p} = \frac{\left( -\frac{b}{\beta} + \frac{\phi_{\Delta}^{\max}}{2\psi_0} \right)}{2 + \frac{\alpha}{a} \frac{\phi_0}{\psi_0}}, \\ \widehat{q} = 0, \\ \widehat{r} = 0. \end{cases}$$

The values  $\widehat{n}, \widehat{p}$  coincide with the values  $\widetilde{n}, \widetilde{p}$  given in (1.9).

After these preliminaries we proceed with the usual calculations. For the sake of simplicity we adopt the notation

$$(5.6) \quad \dot{\vec{x}} = \vec{f}(\vec{x}),$$

with

$$(5.7) \quad \vec{x} = (n, p, q, r), \quad \vec{f} = (f_n, f_p, f_q, f_r)$$

and  $f_i$  are the right-hand side of eq. (5.2). The linear system is

$$(5.8) \quad \dot{\vec{\xi}} = (D\vec{f})_{\vec{x}=\vec{\bar{x}}} \cdot \vec{\xi},$$

where

$$(5.9) \quad \vec{\xi} = \vec{x} - \vec{\bar{x}},$$

and explicitly

$$(5.10) \quad \vec{\xi} = (\xi_n, \xi_p, q, r), \quad \vec{\bar{x}} = (\widehat{n}, \widehat{p}, 0, 0),$$

$\widehat{n}$  and  $\widehat{p}$  are given by (5.5). Finally  $D\vec{f} = \left[ \frac{\partial f_i}{\partial x_j} \right]$  is the Jacobian matrix of the first partial

derivatives of  $\vec{f}$ . Performing the calculation of the Jacobian matrix, we end up with the following system ( $D\vec{f} \equiv A^{(e)}$ ; the index (e) stands for extended):

$$(5.11) \quad \dot{\vec{\xi}} = A^{(e)} \cdot \vec{\xi},$$

where

$$(5.12) \quad A^{(e)} = \begin{pmatrix} a_{11} & a_{12} & a_{13} & 0 \\ a_{21} & a_{22} & 0 & 0 \\ 0 & 0 & 0 & 1 \\ 0 & 0 & -\omega^2 & 0 \end{pmatrix}, \quad A = \begin{pmatrix} a_{11} & a_{12} \\ a_{21} & a_{22} \end{pmatrix}$$

and, explicitly,

$$(5.13) \quad \begin{cases} a_{11} = -2a\hat{n} - \alpha\hat{p} - a\frac{\psi_0}{\phi_0}\hat{p} + \frac{1}{2}a\frac{\phi_A^{\max}}{\phi_0} = -a\hat{n} < 0, \\ a_{12} = -\alpha\hat{n} - a\frac{\psi_0}{\phi_0}\hat{n} < 0, \\ a_{13} = -\varepsilon a\frac{\phi_A^{\max}}{2\phi_0}\hat{n} < 0, \\ a_{21} = \beta\frac{\phi_0}{\psi_0}\hat{p} > 0, \\ a_{22} = -b + \beta\frac{\phi_0}{\psi_0}\hat{n} - 2\beta\hat{p} = -\beta\hat{p} < 0. \end{cases}$$

We perform a linear transformation on the matrix  $A^{(e)}$ , bringing it to a diagonal form:

$$(5.14) \quad \begin{cases} a'_{11} = \lambda_1 = \frac{1}{2}(\text{Tr} A + \sqrt{(\text{Tr} A)^2 - 4 \det A}) \\ a'_{22} = \lambda_2 = \frac{1}{2}(\text{Tr} A - \sqrt{(\text{Tr} A)^2 - 4 \det A}), \\ a'_{33} = \lambda_3 = i\omega, \\ a'_{44} = \lambda_4 = -i\omega, \end{cases}$$

where

$$(5.15) \quad \text{Tr} A = a_{11} + a_{22} < 0, \quad \det A = a_{11} a_{22} - a_{12} a_{21} > 0.$$

(Notice that the eigenvalues of  $A$  do not depend on the perturbation parameter  $\varepsilon$ .) We

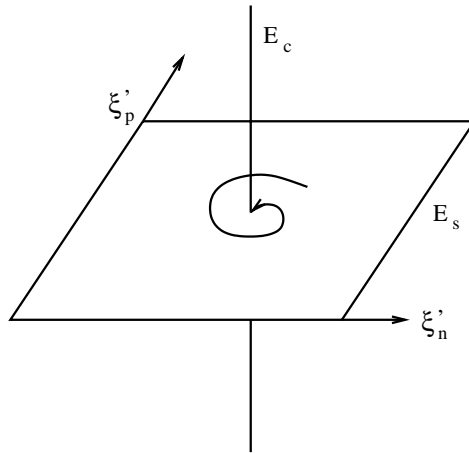


Fig. 7.

see that the eigenvalues  $\lambda_1$  and  $\lambda_2$  are either real negative for

$$(5.16) \quad \frac{(\text{Tr}A)^2}{4} - \det A > 0,$$

or complex with negative real part for

$$(5.17) \quad \det A - \frac{(\text{Tr}A)^2}{4} \equiv \omega_1^2 > 0.$$

The phase portrait of system (5.2) corresponding to the case (5.17) is shown in fig. 7. The center has frequency  $\omega$ , the spiral has frequency  $\omega_1$ . The plane  $\xi_n, \xi_p$  is the stable manifold, the straight line  $E_c$  stands for the two-dimensions center manifold  $q, r$ . We must return from the vector  $\vec{\xi}'$  to the original vector  $\vec{\xi}$ ; this is done, evidently, with the same transformation matrix that has diagonalized  $A$ , therefore the  $\vec{\xi}$  components are a linear combination of  $\vec{\xi}'$  components, and this transformation preserves the property of asymptotic periodicity.

The reader will notice that since in our problem (5.2) the center manifold is linear, because the third and fourth equations are linear, the connection between the nonlinear flow (5.2) and the linear flow (5.11) is trivial, or, in other words, we do not need the use of the center manifold theorem [4]. This is, by the way, a proof of the asymptotic periodicity of  $n(t)$  and  $p(t)$ , equivalent to that given in sect. 1.

### 6. – The resonant behaviour

The analysis of the preceding session suggests the possibility of a resonance between  $\omega_1$  and  $\omega$ . In order to understand the problem, we need a detailed study of the asymptotic solution of system (5.11). Having established the general properties of the 4-dimensional autonomous linear system, we use from now on the short notation of the

two-dimensional linear forced system. We write

$$(6.1) \quad \begin{cases} \dot{x}_1 = a_{11}x_1 + a_{12}x_2 + a_{13} \cos \omega t, \\ \dot{x}_2 = a_{21}x_1 + a_{22}x_2. \end{cases}$$

We call  $A$  the matrix

$$(6.2) \quad A = \begin{pmatrix} a_{11} & a_{12} \\ a_{21} & a_{22} \end{pmatrix},$$

where  $a_{ij}$  are given by (5.13). The relationship between  $x_1$ ,  $x_2$  and  $n$ ,  $p$  is given by

$$(6.3) \quad \begin{cases} n = \widehat{n} - x_1, \\ p = \widehat{p} - x_2. \end{cases}$$

In the asymptotic regime we can take the origin of time as we wish. We have from (5.1)

$$(6.4) \quad \begin{cases} \mathcal{D}(t) = \frac{\phi_A^{\max}}{\phi_0} \frac{1 - \varepsilon \cos \omega t}{2}, \\ \mathcal{D}(t=0) = \mathcal{D}^{\min}, \end{cases}$$

and from (6.1)

$$(6.5) \quad a_{13} \cos \omega(t=0) = a_{13} = -\varepsilon a \frac{\phi_A^{\max}}{2\phi_0} \widehat{n},$$

finally from (6.3)

$$(6.6) \quad \begin{cases} x_1 = x_1^{\max} \rightarrow n = n^{\min}, \\ x_2 = x_2^{\max} \rightarrow p = p^{\min}. \end{cases}$$

We now consider the following particular solution of (6.1):

$$(6.7) \quad \begin{cases} x_1 = \mathcal{A} \cos(\omega t + \varphi_a), \\ x_2 = \mathcal{B} \cos(\omega t + \varphi_b). \end{cases}$$

With the position (6.7), the minimum of  $n$ ,  $p$  comes with the maximum of  $x_1$ ,  $x_2$ , namely

$$(6.8) \quad \begin{cases} x_1 = \mathcal{A}, \\ x_2 = \mathcal{B}, \end{cases}$$

which implies

$$(6.9) \quad \begin{cases} \omega\tau_a + \varphi_a = 0 \rightarrow \tau_a = -\frac{\varphi_a}{\omega}, \\ \omega\tau_b + \varphi_b = 0 \rightarrow \tau_b = -\frac{\varphi_b}{\omega}. \end{cases}$$

In conclusion we have a time advance or delay

$$\begin{aligned} \tau_a > 0 &\rightarrow \varphi_a < 0, \text{ time delay,} \\ \tau_b > 0 &\rightarrow \varphi_b < 0, \text{ time delay,} \\ \tau_a < 0 &\rightarrow \varphi_a > 0, \text{ time advance,} \\ \tau_b < 0 &\rightarrow \varphi_b > 0, \text{ time advance.} \end{aligned}$$

After these preliminaries, we insert (6.7) into (6.1), equate like terms and find

$$(6.10) \quad \begin{cases} \mathcal{A}a_{11} \cos \varphi_a + \mathcal{B}a_{12} \cos \varphi_b + \mathcal{A}\omega \sin \varphi_a = a_{13}, \\ -\mathcal{A}\omega \cos \varphi_a + \mathcal{A}a_{11} \sin \varphi_a + \mathcal{B}a_{12} \sin \varphi_b = 0, \\ \mathcal{A}a_{21} \cos \varphi_a + \mathcal{A}a_{22} \cos \varphi_b + \mathcal{B}\omega \sin \varphi_b = 0, \\ -\mathcal{B}\omega \cos \varphi_b + \mathcal{A}a_{21} \sin \varphi_a + \mathcal{B}a_{22} \sin \varphi_b = 0. \end{cases}$$

The solution is

$$(6.11) \quad \begin{cases} \varphi_a = \arctan \left[ \omega \frac{a_{22} \text{Tr} A - (\det A - \omega^2)}{a_{22}(\det A - \omega^2) + \omega^2 \text{Tr} A} \right] = \varphi_b - \arctan \frac{\omega}{a_{22}}, \\ \mathcal{A} = -\frac{a_{13} \sqrt{a_{22}^2 + \omega^2}}{\sqrt{(\det A - \omega^2)^2 + \omega^2 (\text{Tr} A)^2}} = \varepsilon \mathcal{A}', \\ \varphi_b = \arctan \left[ \frac{\omega \text{Tr} A}{\det A - \omega^2} \right], \\ \mathcal{B} = -\frac{a_{13} a_{21}}{\sqrt{(\det A - \omega^2)^2 + \omega^2 (\text{Tr} A)^2}} = \varepsilon \mathcal{B}'. \end{cases}$$

From (6.11) we see first of all how the cut-off parameter  $\varepsilon$  works. In fact, given a set of values  $a, \phi_0, z, \alpha, \gamma$ , the amplitudes  $\mathcal{A}'$  and  $\mathcal{B}'$  are determined, and, correspondingly, we may evaluate  $\hat{n} - \mathcal{A}, \hat{p} - \mathcal{B}$ . When the straight line  $\mathcal{A} = \varepsilon \mathcal{A}'$  (or  $\mathcal{B} = \varepsilon \mathcal{B}'$ ) reaches the value  $\hat{n}$  (or  $\hat{p}$ ) we get a critical value  $\varepsilon = \varepsilon_c$ , which is the value that must be used in (5.1) in order to avoid unphysical values in the phase space  $n, p$ . In fig. 8-10, we show the situation for two values of  $z$ .

The comparison of fig. 8 and 9 with 5 and 6 shows that the linearized system is not a completely faithful representation of the nonlinear system, as long as shape and size of the analytic solutions are concerned.

Next we consider the time displacement. For the nonlinear system the driving term is sinusoidal, while  $n(t)$  and  $p(t)$  are oddly shaped. We define the time displacement  $\tau_{\text{dn}}$

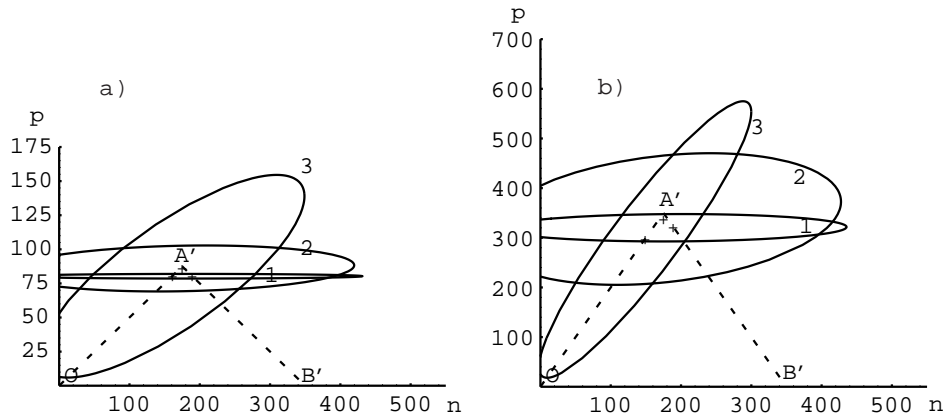


Fig. 8. - Three trajectories in the phase space, with  $n$  and  $p$  solutions of the linearized system (6.1), (6.3) with  $\gamma = 0.9$ , for  $z = 2$  (a) and for  $z = \frac{1}{2}$  (b). 1) Weak coupling:  $\alpha = 0.1 \hat{\alpha}_0$ , the fixed point is the cross on the right-hand side of  $A'$ . 2) Maximum predator:  $\alpha = \hat{\alpha}_0$ , the fixed point is the cross almost coincident with  $A'$ . 3) Strong coupling  $\alpha = 10 \hat{\alpha}_0$ , the fixed point is the cross on the left-hand side of  $A'$ . Compare this plot with fig. 5.

the distance in time between the time at which  $n$  is maximum and the time at which  $\mathcal{D}$  is maximum. Similarly for  $p$ :

$$(6.12) \quad \begin{cases} \tau_{dn} = t_{n \max} - t_{d \max}, \\ \tau_{dp} = t_{p \max} - t_{d \max}, \end{cases}$$

$\tau_{dn}$  and  $\tau_{dp}$  can be calculated numerically. For the linear system both the driving term and the solution  $n, p$  are sinusoidal and therefore the time displacement is simply related to the frequency of the input  $\omega$  by a fixed angular displacement, as we pointed out with (6.9):

$$(6.13) \quad \varphi_a = \omega \tau_a, \quad \varphi_b = \omega \tau_b.$$

We can use a dimensionless quantity, in analogy with (6.13), also for the nonlinear case,

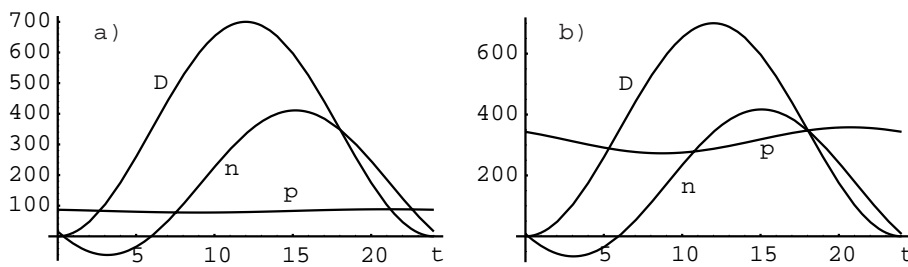


Fig. 9. - Asymptotic regime in the reference case:  $\alpha = \hat{\alpha}_0, \gamma = 0.5$ , for  $z = 2$  (a) and for  $z = \frac{1}{2}$  (b). The solutions of the linearized system (6.1), (6.3),  $n$  and  $p$ , are plotted together with the input term  $\mathcal{D}(t)$  (eq. (1.2)). Compare this graph with fig. 6. Time is expressed in hours.



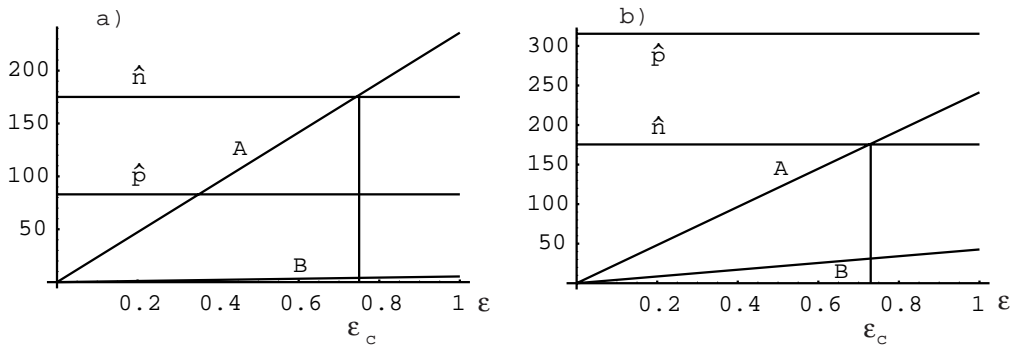


Fig. 10. -  $\hat{n}$ ,  $\hat{p}$ ,  $A$ ,  $B$  as a function of  $\epsilon$ . We have chosen  $\alpha = \hat{\alpha}_0$ ,  $\gamma = 0.5$ ,  $z = 2$  (a) and  $z = 0.5$  (b).

and we define the nonlinear phase shifts:

$$(6.14) \quad \varphi_{dn} = \omega \tau_{dn}, \quad \varphi_{dp} = \omega \tau_{dp}.$$

We can compare the phase shifts (6.14), calculated numerically, with the angular displacement (6.13), calculated analytically. The result is shown in fig. 11. This shows that the linearization is excellent as far as the reproduction of the phase shifts is concerned.

Finally, we consider the resonant behaviour.

The matrix  $A$  has two real negative eigenvalues for

$$(6.15) \quad \frac{(\text{Tr} A)^2}{4} - \det A > 0 \quad \rightarrow \quad \lambda_{1,2} = \frac{1}{2} \text{Tr} A \pm \sqrt{\frac{(\text{Tr} A)^2}{4} - \det A}$$

and two complex conjugate eigenvalues for

$$(6.16) \quad \det A - \frac{(\text{Tr} A)^2}{4} > 0 \quad \rightarrow \quad \lambda_{1,2} = \frac{1}{2} \text{Tr} A \pm i \sqrt{\det A - \frac{(\text{Tr} A)^2}{4}}.$$

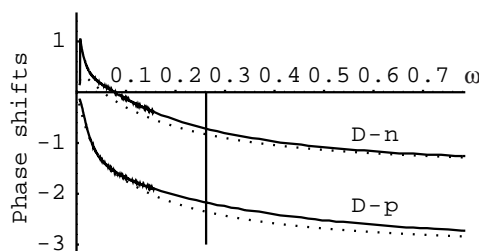


Fig. 11. - Phase shifts  $\varphi_a$  and  $\varphi_b$  (eq. (6.11), dotted lines) compared to the phase shifts  $\varphi_{dn}$ ,  $\varphi_{dp}$  numerically calculated from the nonlinear system (5.1) as a function of  $\omega$  (in  $\text{h}^{-1}$ ). In this calculation we have chosen  $\alpha = \hat{\alpha}_0$ ,  $\gamma = 0.5$ ,  $z = 2$ . The vertical line indicates the value  $\omega = \omega_{\text{day}} = \frac{2\pi}{24} \text{h}^{-1}$ .

In this second case, the linear system contains the inner frequency

$$(6.17) \quad \omega_1 = \sqrt{\det A - \frac{(\text{Tr } A)^2}{4}}.$$

Now we consider the behaviour of  $\mathcal{A}$  and  $\mathcal{B}$  given in (6.11) as functions of  $\omega$ .  $\mathcal{B}$  has a peak for the value of  $\omega$  that satisfies

$$(6.18) \quad \frac{\partial \mathcal{B}}{\partial \omega} = 0, \quad \omega_b = \sqrt{\det A - \frac{(\text{Tr } A)^2}{2}},$$

while the peak of  $\mathcal{A}$  ( $\frac{\partial \mathcal{A}}{\partial \omega} = 0$ ) occurs for

$$(6.19) \quad \omega_a = \sqrt{-a_{22}^2 + \sqrt{(a_{22}^2 + \det A)^2 - a_{22}^2 (\text{Tr } A)^2}}.$$

How this situation compares with a genuine resonance?

*Resonance for the driven dissipative harmonic oscillator.*

We consider the system that defines the concept of resonance: the dissipative driven harmonic oscillator. The equation of motion is

$$(6.20) \quad \ddot{x} + \nu \dot{x} + \omega_0^2 x = d \cos \omega t.$$

This equation may represent the spring in a dissipative medium or a  $L, C, R$  electric circuit. In the first case  $x$  is the elongation of the unit mass point,  $\nu$  is the friction coefficient,  $\omega_0^2$  is the constant of the spring. In the second case  $x$  is the electric charge,  $\nu = \frac{R}{L}$  and  $\omega_0^2 = \frac{1}{LC}$ . In the absence of friction,  $\nu = 0$ , and in the absence of the driving force, the problem is Hamiltonian:

$$(6.21) \quad \ddot{x} = -\omega_0^2 x,$$

with potential

$$(6.22) \quad U = \frac{1}{2} \omega_0^2 x^2,$$

and a conserved total energy:

$$(6.23) \quad E = \frac{1}{2} \dot{x}^2 + \frac{1}{2} \omega_0^2 x^2.$$

Equation (6.20) can be written in the form of a system of two first-order equations introducing the two variables

$$(6.24) \quad \begin{cases} x_1 = \dot{x}, \\ x_2 = x; \end{cases}$$

in this way we obtain

$$(6.25) \quad \begin{cases} \dot{x}_1 = -\nu x_1 - \omega_0^2 x_2 + d \cos \omega t, \\ \dot{x}_2 = x_1. \end{cases}$$

System (6.25) is evidently in the form (6.1). The first important observation is that in the case of the genuine resonance the matrix  $A$  has the form

$$(6.26) \quad A = \begin{pmatrix} a_{11} & a_{12} \\ 1 & 0 \end{pmatrix}.$$

From this fact follows that the original variable is  $x = x_2$ , while  $x_1$  is an auxiliary variable related to  $x_2$  by a derivative,  $x_1 = \dot{x}_2$ . In Hamiltonian language  $x_2$  is the coordinate,  $x_1$  is the momentum.

The second observation comes by writing explicitly the matrix elements  $a_{ij}$ :

$$(6.27) \quad A = \begin{pmatrix} -\nu & -\omega_0^2 \\ 1 & 0 \end{pmatrix}, \quad a_{11} = -\nu, \quad a_{12} = -\omega_0^2, \quad a_{21} = 1, \quad a_{22} = 0, \quad \text{and} \quad a_{13} = d.$$

We have

$$(6.28) \quad \text{Tr} A = -\nu, \quad \det A = \omega_0^2.$$

The eigenvalues of  $A$  are either real negative:

$$(6.29) \quad \lambda_{1,2} = -\frac{\nu}{2} \pm \sqrt{\frac{\nu^2}{4} - \omega_0^2},$$

or complex conjugate:

$$(6.30) \quad \lambda_{1,2} = -\frac{\nu}{2} \pm i\omega_1,$$

and

$$(6.31) \quad \omega_1 = \sqrt{\omega_0^2 - \frac{\nu^2}{4}}.$$

The  $\text{Tr} A$  contains the friction, the  $\det A$  contains the inner frequency, namely the Hamiltonian part of the problem.  $\text{Tr} A$  and  $\det A$  are independent of each other. The general solution (6.11), valid for a generic matrix  $A$ , becomes, by direct application of

(6.27), (6.28),

$$(6.32) \quad \left\{ \begin{aligned} \varphi_a &= \arctan \left[ \frac{\omega_0^2 - \omega^2}{\nu\omega} \right] = \varphi_b + \frac{\pi}{2}, \\ \mathcal{A} &= - \frac{\omega d}{\sqrt{(\omega_0^2 - \omega^2)^2 + \nu^2 \omega^2}}, \\ \varphi_b &= \arctan \left[ \frac{-\nu\omega}{\omega_0^2 - \omega^2} \right], \\ \mathcal{B} &= - \frac{d}{\sqrt{(\omega_0^2 - \omega^2)^2 + \nu^2 \omega^2}}. \end{aligned} \right.$$

In particular, the limit of no dissipation,  $\nu \rightarrow 0$  ( $\omega_1 \rightarrow \omega_0$ ), is physically conceivable, because  $\nu$  and  $\omega_0$  are independent of each other. The maximum of  $\mathcal{B}$  (solution of  $\frac{d\mathcal{B}}{dt} = 0$ ) occurs at the value

$$(6.33) \quad \omega_b = \sqrt{\det A - \frac{(\text{Tr } A)^2}{2}} = \sqrt{\omega_0^2 - \frac{\nu^2}{2}},$$

while the maximum of  $\mathcal{A}$  (solution of  $\frac{d\mathcal{A}}{dt} = 0$ ) occurs at the value

$$(6.34) \quad \omega_a = \sqrt{\det A} = \omega_0.$$

We have

$$(6.35) \quad \omega_0 > \omega_1 > \omega_b.$$

Final remark. To see a peak in the amplitude  $\mathcal{B}$ , we need  $\omega_b > 0$ , and this implies the condition of complex eigenvalues of  $A$ , namely  $\omega_1 > 0$ . On the other hand, the auxiliary amplitude  $\mathcal{A}$  has always a peak, even if the constraint  $\omega_1 > 0$  is not satisfied. In fact, in this case,  $\mathcal{B}$  is a monotonous decreasing function of  $\omega$  and  $\mathcal{A}$  is the product  $\omega\mathcal{B}$ , therefore has a maximum for  $\omega = \omega_0$ . This situation is summarized in fig. 12, where we show in the parameter space the domains in which  $\omega_1 > 0$ ,  $\omega_b > 0$ ,  $\omega_a > 0$ . Inside the domain  $D_a$  there is a peak of  $\mathcal{A}$  but no complex eigenvalues.

We compare now these results to the properties of the ecosystem equation (6.1). In the ecosystem case,  $x_1$  and  $x_2$  have independent physical meanings,  $x_1$  is the prey and  $x_2$  is the predator. They are no longer simply related as coordinate and momentum. In the ecosystem case there is no  $\det A$  independent of  $\text{Tr } A$ , or, in other words, no proper frequency independent of friction. We may call

$$(6.36) \quad \text{Tr } A = -a\hat{n} - \beta\hat{p}$$

the friction of the ecosystem, if we wish, but such generalized friction is a rather complex function of the parameters. Similarly we may call

$$(6.37) \quad \det A = a\beta\hat{n}\hat{p} + \beta \frac{\phi_0}{\psi_0} \hat{p} \left( a\hat{n} + a \frac{\psi_0}{\phi_0} \hat{n} \right) = \omega_0^2$$

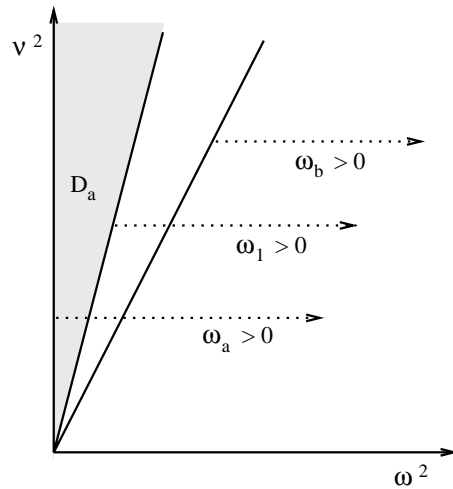


Fig. 12.

the proper frequency, but such generalized frequency is a rather complex function of the parameters. Moreover the matrix element  $a_{22} = -\beta\hat{p}$  cannot be considered negligible, because the limit  $a_{22} \rightarrow 0$  implies  $\hat{p} \rightarrow 0$ , in other words  $\text{Tr}A$  and  $\text{det}A$  are uncoupled only if one component, the predator, disappears. For this reason the ideal limit of vanishing friction does not exist.

In the ecosystem, we have that the condition that must be satisfied in order to have a sufficiently narrow peak in the amplitudes  $\mathcal{A}$  and  $\mathcal{B}$  is a constraint in the multidimensional parameter space. We have already noticed that  $\phi_0$  simply gives the scale in the variable  $n$ . We may choose a typical value for  $a$  and  $z$ , in this way we are left

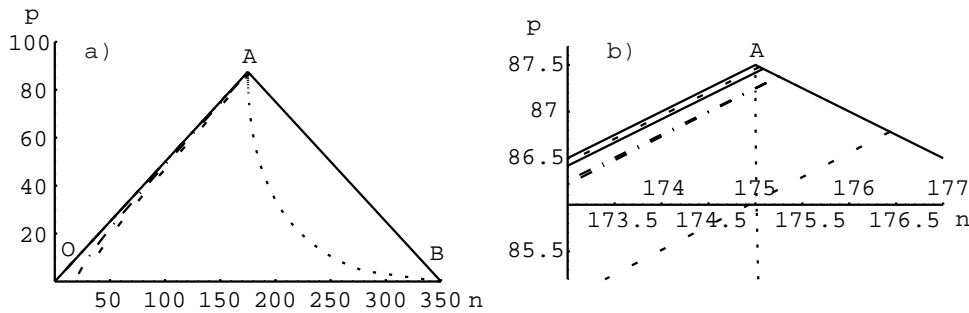


Fig. 13. – The resonant domain in phase space. The curve  $n(\gamma_{a1}(\alpha)), p(\gamma_{a1}(\alpha))$  (continuous line); the curves  $n(\gamma_{b1}(\alpha)), p(\gamma_{b1}(\alpha))$  and  $n(\gamma_{b2}(\alpha)), p(\gamma_{b2}(\alpha))$  (dash-dotted lines), almost indistinguishable; the curves  $n(\gamma_{c1}(\alpha)), p(\gamma_{c1}(\alpha))$  and  $n(\gamma_{c2}(\alpha)), p(\gamma_{c2}(\alpha))$  (dashed lines) and the curve  $n(\alpha_0(\gamma)), p(\alpha_0(\gamma))$  (dotted line). Concerning the last, it begins at  $B$  for  $\gamma = 0$  and ends at  $A$  for  $\gamma = 1$ .

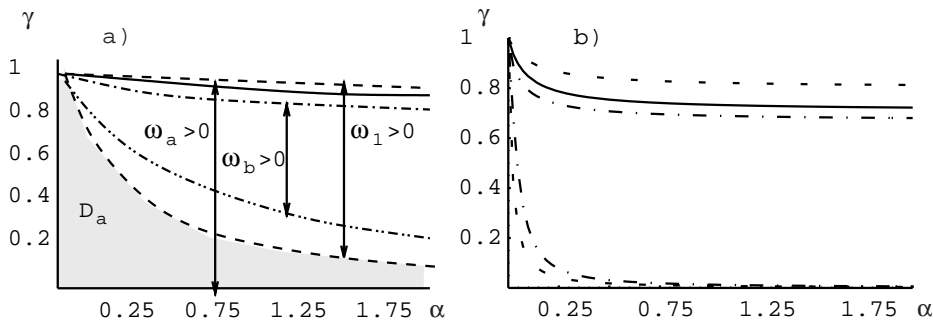


Fig. 14. – The resonant domain in the parameter space (a)  $z = 2$ ; b)  $z = 0.1$ . Curves  $\gamma_{a1}(\alpha)$  (continuous line),  $\gamma_{b1}(\alpha)$ ,  $\gamma_{b2}(\alpha)$  (dash-dotted lines)  $\gamma_{c1}(\alpha)$ ,  $\gamma_{c2}(\alpha)$  (dashed lines) plotted in the parameter space, as a function of  $\alpha$  (in units of  $a$ ) and  $\gamma$ . In the domain  $D_a$  there is a peak of  $\mathcal{A}$  (dimensionless), but no complex eigenvalues.

with two free parameters,  $\alpha$  and  $\gamma$ . We therefore find that the constraint

$$(6.38) \quad \det A \geq \frac{(\text{Tr } A)^2}{2}$$

selects the region in the parameter space in which  $\mathcal{B}$  shows a resonant behaviour. Equation (6.38) is of the kind  $F(\alpha, \gamma) > 0$ , namely is a constraint on the variables  $\alpha, \gamma$ . In particular we find that the condition (6.38) is satisfied for

$$(6.39) \quad \gamma_{b1}(\alpha) \leq \gamma \leq \gamma_{b2}(\alpha), \quad \omega_b > 0.$$

The amplitude  $\mathcal{A}$  has a peak in  $\omega_a$  (eq. (6.19)) if

$$(6.40) \quad \det A \geq a_{22}^2 \left( \sqrt{1 + \frac{(\text{Tr } A)^2}{a_{22}^2}} - 1 \right),$$

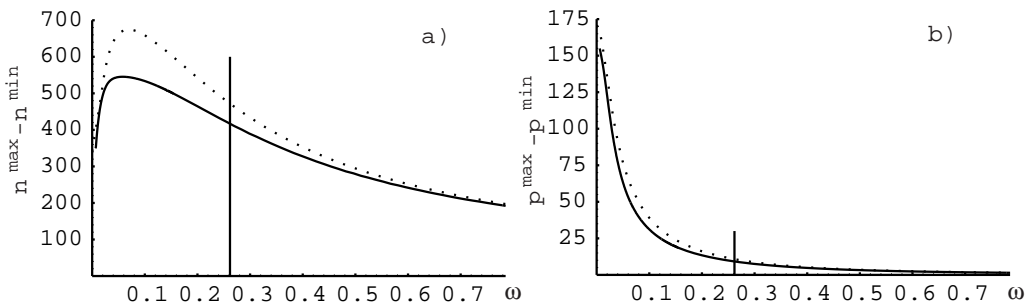


Fig. 15. – The excursions  $2\mathcal{A}$  and  $2\mathcal{B}$  (eq. (6.11), dotted lines) compared to those numerically calculated from the nonlinear system (5.1) as a function of  $\omega$  (in  $\text{h}^{-1}$ ). In this calculation we have chosen  $\alpha = \hat{\alpha}_0$ ,  $\gamma = 0.5$ ,  $z = 2$ . The vertical line indicates the value  $\omega = \omega_{\text{day}} = \frac{2\pi}{24} \text{h}^{-1}$ .

that is satisfied for

$$(6.41) \quad \gamma \leq \gamma_{a1}(\alpha), \quad \omega_a > 0.$$

Moreover, the eigenvalues are complex, when

$$(6.42) \quad \det A \geq \frac{(\text{Tr} A)^2}{4},$$

that gives

$$(6.43) \quad \gamma_{c1}(\alpha) \leq \gamma \leq \gamma_{c2}(\alpha), \quad \omega_1 > 0.$$

The curves  $\gamma_a(\alpha)$ ,  $\gamma_b(\alpha)$ ,  $\gamma_c(\alpha)$  delimiting these regions, can be calculated analytically. The results are plotted in fig. 13, in the phase space and, in fig. 14, in the parameter space. Notice the analogy between fig. 12 and fig. 14. In both cases the domain  $\omega_b$  is contained in the domain  $\omega_1$ , and the domain  $\omega_a$  has a sub-domain  $D_a$  external to the domain of complex eigenvalues. Finally the region of low predator efficiency  $\gamma$  corresponds to the region of high friction  $\nu$ .

The last comment about the linearization concerns the description of the amplitudes of the oscillations of  $n$  and  $p$ . This is shown in fig. 15. This figure indicates that the linear system is a faithful tool in the understanding of the reason why in certain regions of the parameters space the amplitudes of the oscillations of  $n$  and  $p$  are particularly large.

\* \* \*

We thank Prof. CESARE ROSSETTI for several stimulating discussions. We thank also dr. PATRICK DE LEENHEER for having brought to our attention the book of Verhulst.

## REFERENCES

- [1] SERTORIO L. and TINETTI G., *Prey-Predator Dynamics driven by the Solar Radiation* (Preprint DFTT 72/99, Dipartimento di Fisica Teorica, Università di Torino).
- [2] ARNOLD V. I., *Matematicheskie Metody Klassiceskoj Mehaniki* (MIR, Mosca) 1979; VERHULST F., *Nonlinear Differential Equations and Dynamical Systems* (Springer-Verlag) 1996.
- [3] WEST G. B., BROWN J. H. and ENQUIST B. J., *Allometric Scaling Laws in Biology Science*, **276** (1997) 122-126.
- [4] GUCKENHEIMER J. and HOLMES P., *Nonlinear Oscillations, Dynamical Systems, and Bifurcations of Vector Fields* (Springer-Verlag New York) 1983.